Muti-omics revealed the global response of Hordeum vulgare to different wavelength of UV exposure

Zhihua Hao
Xizang Academy of Agricultural and Animal Husbandry Sciences
Xiaojun Yang
Xizang Academy of Agricultural and Animal Husbandry Sciences
Ciren Deji
Xizang Academy of Agricultural and Animal Husbandry Sciences
Yifan Zhang
Xizang Academy of Agricultural and Animal Husbandry Sciences
Xuelian Wu
Xizang Academy of Agricultural and Animal Husbandry Sciences
Ying Li
Xizang Academy of Agricultural and Animal Husbandry Sciences
Ci Dun
Xizang Academy of Agricultural and Animal Husbandry Sciences
Tangwei Zhang
zhangtangwei04@163.com

Xizang Academy of Agricultural and Animal Husbandry Sciences

Research Article

Keywords: Hordeum vulgare, Multi-omics, UV exposure, Regulation network, Transcription factor, Anthocyanin biosynthesis

Posted Date: April 23rd, 2025

DOI: https://doi.org/10.21203/rs.3.rs-5763885/v1

Additional Declarations: No competing interests reported.

Abstract

Background

UV seriously affected *Hordeum vulgare* growth, which limited the its development and production in the plateau region. However, the detailed response mechanisms of *Hordeum vulgare* to UV exposure remain unclear.

Results

We found that UVA, UVAB and UVB reprogrammed the proteome pattern of *H. vulgare*. UVA mainly affected the expression of proteins involved in cell cycle and DNA repair, while UVB and UVAB mainly activated proteins involved in anthocyanin biosynthesis and antioxidant systems, leading to accumulation of anthocyanin in *H. vulgare*. Then, we constructed the network for regulating UV-triggered anthocyanin biosynthesis in *H. vulgare* using proteome profiles. Importantly, we identified that NAC transcription together with numerous kinases were responsible for regulating UVAB/UVB-triggered anthocyanin biosynthesis in *H. vulgare*. Of note, NAC1 directly bound on the promoters of *CAD1* and *CHS* to trigger their expression, then activated anthocyanin biosynthesis in *H. vulgare*.

Conclusions

Our research gain insight into the global responses of *H. vulgare* to UV exposures, then provided guidance for protecting plant from UV stress in plateau.

Introduction

Plants are often challenged by numerous adverse abiotic stresses, including drought, high salinity, and especially UV exposure (i.e., UVA and UVB) [1]. With the increasingly prominent global environmental changes, the increasing trend of ultraviolet radiation is becoming more and more obvious. Studies have shown that the ultraviolet radiation on the Earth's surface has increased by 6–14% and will continue to increase in the future [2]. UV-B is the ionizing radiation with a wavelength of 280 to 315 nm that can penetrate the ozone layer and is a part of the solar radiation. In recent years, with the decrease of the ozone layer, UV-B radiation reaching the Earth's surface has increased [3, 4]. High doses of UV-B damage amino acid residues, leading to protein and enzyme inactivation of amino acids in synthesis [5, 6]. Studies have shown that UV-B radiation can significantly inhibit the photosynthetic rate of plants, hinder plant growth and development, and lead to a decrease in crop yield [7–10]. Highland barley (*Hordeum vulgare* L.) is a kind of Chinese general name for naked barley in the Tibetan plateau area, and always challenged by strong UV challenge in production region. Typically, highland barley has the advantages of drought resistance, cold resistance, UV resistance and humidity resistance, which lead to it adapted to plant in a range of Tibetan plateau area. Thus, it has been the most important food crop for farmers and

herdsmen in Tibetan areas. At present, China's highland barley planting area is about 333,300 hm^2, 95% of which is distributed in the Qinghai-Tibet Plateau, while Tibet's highland barley planting area is the largest, highest yield, and most widely distributed, its planting area is about 240,000 hm^2, accounting for 72% of the major planting area. Moreover, the proportion of grain crop planting area and output in the whole region has always remained above 70%. Thus, understanding the detailed responses of plants to UV exposure is of great significance for their development and cultivation.

In order to cope with the harsh living environment, plants growing on the Qinghai-Tibet Plateau show different adaptive traits, such as the shape and color of roots, stems and leaves, the interaction between different plants, and the change of reproduction mode [11, 12]. Typically, plant altered the expression levels of soluble sugar, superoxide dismutase, peroxidase, etc., in the leaf tissues to strong ultraviolet radiation in the Qinghai-Tibet Plateau, and the physiological characteristics of plants are transformed to protect plants from UV exposure [11]. In addition, wild barley on the plateau mainly changed genes related to DNA damage repair, nitrogen metabolism, cell membrane stability regulation, UV radiation resistance and other functions, so as to adapt to excessive UV radiation on the Qinghai-Tibet Plateau [11]. It has shown that UV-B exerted significant effect on gene expression related to the biosynthesis of plant secondary metabolites [12, 13], in which increased accumulation of secondary metabolites in plants [14]. These secondary metabolites include terpenoids [15], alkaloids, and phenols [16].and secondary nitrogen-containing compound [17]. Flavonoids also exerted many important physiological effects on plants, especially protecting plants from biotic and abiotic stresses [18]. Recently, it was found that UV radiation significantly affected the compositions of flavonoids and anthocyanins in plant [19, 20]. Park et al. (2008) [21] found that the synthesis of plant flavonoids and anthocyanins is related to many factors, typically their synthetic genes are affected by UV-B radiation [21]. In detail, flavonoids can accumulate in some special parts of plant cells, such as cell walls, vacuoles, chloroplasts, and glands [21]. Additionally, the contents of flavonoids and anthocyanins in *C. mongolica* and *Cymbopogon citratus* were significantly increased after UV-B stress [22–24]. Anthocyanins are distributed in plant epidermal cells, while numerous structural genes and transcription factors play an important role in the synthesis of anthocyanins and flavonoids [25]. Ohnishi et al. (1992) [26] found that anthocyanin could inhibit DNA damage in *Centaurea cyanus* under the condition of UV-B increase, thus protecting the normal growth and development of plants under UVB condition. However, the detailed metabolic compositions in Hordeum vulgare under different wavelength of UV exposures remained unclear.

Hordeum vulgare, which is widely distributed in habitat, is always exposed under UV challenges, however its detailed responses to UV exposure remain unclear. In this study, we deployed 4-D proteome and anthocyanins metabolomics to investigate the responses of *Hordeum vulgare* to different wavelength and composition of UV exposures, including UVA, UVAB and UVB. It was found that UVA, UVAB, and UVB exposures caused different responses in *H. vulgare* at proteome levels. Typically, *H. vulgare* reprogrammed anthocyanins biosynthesis to accumulated more related metabolites in response to UVAB and UVB exposures. And NAC1 was responsible for activating anthocyanin biosynthesis of *H. vulgare* in response to UV exposure. Overall, our research depicted global proteome and anthocyanins

landscape of *H. vulgare* under different wavelength of UV exposures, which contributed to the cultivation and management of *H. vulgare* from UV stress, especially in plateau.

Materials and Methods

Sample preparation

Here, Longzi black highland barley, a variety of black highland barley rich in anthocyanins, was planted in pots with vegetative soil as the substrate. Totally, 120–130 seedlings were planted in each pot at Xizang Academy of Agricultural and Animal Husbandry Sciences experimental fields. Plants were grown in a greenhouse at a temperature of 20°C/day and 15°C/night, and watered every 5 days. The highland barley was subjected to ultraviolet stress at the earing stage. Each treatment was divided into experimental group and control group. Typically, three kinds of UV stress treatments were set up and compared with P normal sunlight exposure, treatment 1 was PA (sunlight P + UVA 400-320nm), treatment 2 was PB (sunlight P + UVB 320-280nm), treatment 3 was PAB (sunshine P + UVA + UVB) mixed irradiation, treatment for 8 hours a day, treatment for 8 days, control for outdoor planting, three parallel treatments, a total of 36 samples. The information of UV-B light is 5.5 W cm^{-2}, equivalent to 12 μmol m^{-2} s^{-1} (measured by a UV-297 UV-B Light Meter, HANDY) provided by Philips TL20W/01RS narrowband UV-B tubes11. And the information of UV-A light is 5.5 W m^{-2}, PPFD = 12 μmol·m^{-2} s^{-1}, as measured by a portable digital radiometer for UV (UV-340A, Lutron, Taiwan).

Protein extraction and digestion

To investigate the responses of *Hordeum vulgare* to UVA, UVAB and UVB exposure, three biological replicates of *H. vulgare* were collected from all experimental groups (UVA, UVAB and UVB) for proteome analysis. Sample analysis and protein extraction were performed using SDT (4% SDS, 100 mM Tris-HCl, 1 mM DTT, pH 7.6) buffer and quantified with the BCA Protein Assay Kit (BioRad, Hercules, CA, USA). Then, the protein was digested by trypsin and desalted on C18 cartridges (Empore™ SPE Cartridges C18 (standard density), bed I.D. 7 mm, volume 3 mL, Sigma, Burlington, MA, USA), concentrated via vacuum centrifugation and reconstituted in 40 μL of 0.1% (v/v) formic acid. Filter-aided sample preparation (FASP digestion) procedure: 200 μg of protein for each sample was incorporated into 30 μL SDT buffer (4% SDS, 100 mM DTT, 150 mM Tris-HCl pH 8.0). The detergent, DTT and other low-molecular-weight components were removed using UA buffer (8 M urea, 150 mM Tris-HCl pH 8.0) via repeated ultrafiltration (Microcon units, 10 kD). Then, 100 μL iodoacetamide (100 mM IAA in UA buffer) was added to block reduced cysteine residues and the samples were incubated for 30 min in darkness. The filters were washed with 100 μL UA buffer three times and then 100 μL 25 mM NH_4HCO_3 buffer twice. Finally, the protein suspensions were digested with 4 μg trypsin (Promega) in 40 μL 25 mM NH_4HCO_3 buffer overnight at 37°C, and the resulting peptides were collected as a filtrate. The peptides of each sample were desalted on C18 cartridges (Empore™ SPE Cartridges C18 (standard density), bed I.D. 7 mm, volume 3 mL, Sigma, Burlington, MA, USA), concentrated via vacuum centrifugation and reconstituted in

40 µL of 0.1% (v/v) formic acid. The peptide content was estimated based on the UV light at 280 nm using an extinction coefficient of 1.1 of 0.1% (g/L) solution that was calculated based on the frequency of tryptophan and tyrosine in vertebrate proteins according to Cheng et al. (2020)[27].

LC-MS/MS detection for proteome analysis

For each sample, 200 ng of total peptides were separated and analyzed with a nanoUPLC (Evosep one) coupled to a timsTOF Pro2 instrument (Bruker) with a nanoelectrospray ion source. Separation was performed using a reversedphase column (PePSep C18, 1.9 µ, 150 µ × 15 cm, Bruker, Germany). Mobile phases were H_2O with 0.1% FA (phase A) and CAN with 0.1% FA (phase B). Separation of sample was executed with a 44 min gradient. The mass spectrometer adopts DDA PaSEF mode for DDA data acquisition, and the scanning range is from 100 to 1700 m/z for MS1. During PASEF MS/MS scanning, the impact energy increases linearly with ion mobility, from 20 eV ($1/K_0$ = 0.6 Vs/cm^2) to 59 eV ($1/K_0$ = 1.6 Vs/cm^2).

SpectroMine database search

Vendor's raw MS files were processed using SpectroMine software (4.2.230428.52329) and the builtin Pulsar search engine. MS spectra lists were searched against their specieslevel UniProt FASTA databases (uniprotkb_Hordeum vulgare_id_4513_2024_05_17), Carbamidomethyl [C] as a fixed modification, Oxidation (M) and Acetyl (Protein Nterm) as variable modifications. Trypsin was used as proteases. A maximum of 2 missed cleavage (s) was allowed. The false discovery rate (FDR) was set to 0.01 for both PSM and peptide levels. Peptide identification was performed with an initial precursor mass deviation of up to 20 ppm and a fragment mass deviation of 20 ppm. All the other parameters were reserved as default.

Bioinformatic Analysis

CELLO v2.5 (http://cello.life.nctu.edu.tw/ accessed on 31 July 2022), a multi-class SVM classification system, was used to predict protein subcellular localization. The protein sequences of the selected differentially expressed proteins were locally searched using the NCBI BLAST + client software (ncbi-blast-2.2.28+-win32.exe) and InterProScan-5.25-64.0 to find homologue sequences, then, gene ontology (GO) terms were mapped and sequences were annotated using the software program Blast2GO 6.0. The GO annotation results were plotted by R scripts. The BLAST2GO 6.0 software was used to perform functional annotation following Ye et al. (2006) [28]. The DEPs of each comparison were mapped to the Kyoto Encyclopedia of Genes and Genomes (KEGG) database (http://www.genome.jp/kegg/ accessed on 31 July 2022) [29]. GO and KEGG pathway enrichment analyses were performed by clusterprofiler 2.0. Only functional categories and pathways with p-values under a threshold of 0.05 were considered significant. Proteins with P-value < 0.05 & $|\log_2(\text{Foldchange})| > 1$ was set as the threshold for significantly

differential expression (Table S4). WGCNA was performed using R package WGCNA following Du et al. (2023) [30]. The detailed information of proteome data were listed in Table S4.

Anthocyanin preparation and extraction

Each experimental group contained three biological replicates to ensure the validity of altitude-induced metabolic changes in *H. vulgare*. Totally, 20 mg of each *H. vulgare* sample from CK, UVA, UVB and UVAB groups was weighted to an EP tube after grinding with liquid nitrogen, and 1000 μL extract solution (methanol: water = 3: 1, with isotopically-labelled internal standard mixture) was added. The sample was freeze-dried, ground into powder (30 Hz, 1.5 min), and stored at -80°C until needed. 50 mg powder was weighted and extracted with 0.5 mL methanol/water/hydrochloric acid (500:500:1, V/V/V). Then the extract was vortexed for 5 min and ultrasound for 5 min and centrifuged at 12, 000 g under 4°C for 3 min. The residue was re-extracted by repeating the above steps again under the same conditions. The supernatants were collected, and filtrated through a membrane filter (0.22 μm, Anpel) before LC-MS/MS analysis. All of the standards were purchased from isoReag (Shanghai, China). Formic acid was purchased from Sigma-Aldrich (St Louis, MO, USA). Hydrochloric acid was bought from Xinyang ChemicalReagent (China). The stock solutions of standards were prepared at the concentration of 1 mg/mL in 50% MeOH. All stock solutions were stored at -20°C. The stock solutions were diluted with 50% MeOH to working solutions before analysis.

LC–MS/MS Analysis for anthocyanin determination

HPLC-grade methanol (MeOH) was purchased from Merck (Darmstadt, Germany). MilliQ water (Millipore, Bradford, USA) was used in all experiments. The sample extracts were analyzed using an UPLC-ESI-MS/MS system (UPLC, ExionLC™ AD, https://sciex.com.cn/, MS, Applied Biosystems 6500 Triple Quadrupole, https://sciex.com.cn/). The analytical conditions were as follows, UPLC: column, WatersACQUITY BEH C18 (1.7 μm, 2.1 mm*100 mm), solvent system, water (0.1% formic acid): methanol (0.1% formic acid), gradient program, 95:5 V/V at 0 min, 50:50 V/V at 6 min, 5:95 V/V at 12 min, hold for 2 min, 95:5 V/V at 14 min, hold for 2 min, flow rate, 0.35 mL/min, temperature, 40°C, injection volume, 2 μL.

Linear ion trap (LIT) and triple quadrupole (QQQ) scans were acquired on a triple quadrupole-linear ion trap mass spectrometer (QTRAP), QTRAP® 6500 + LC-MS/MS System, equipped with an ESI Turbo Ion-Spray interface, operating in positive ion mode and controlled by Analyst 1.6.3 software (Sciex). The ESI source operation parameters were as follows: ion source, ESI+, source temperature 550°C, ion spray voltage (IS) 5500 V, curtain gas (CUR) was set at 35 psi, respectively. Anthocyanins were analyzed using scheduled multiple reaction monitoring (MRM). Data acquisitions were performed using Analyst 1.6.3 software (Sciex). Multiquant 3.0.3 software (Sciex) was used to quantify all metabolites. Mass spectrometer parameters including the declustering potentials (DP) and collision energies (CE) for individual MRM transitions were done with further DP and CE optimization. A specific set of MRM transitions were monitored for each period according to the metabolites eluted within this period.

Data Preprocessing and Annotation

The raw data of all samples were converted to the mzXML format using ProteoWizard and processed with an in-house program, which was developed using R and based on XCMS, for peak detection, extraction, alignment, and integration. Then an in-house MS2 database (BiotreeDB) was applied in metabolite annotation. The cutoff for annotation was set at 0.3. The data variation was performed by R packages XCMS software [31]. The Principal Component Analysis (PCA) was performed using Metaboanalyst 3.0 based on the normalized peak area of the metabolites in each sample. Significantly regulated metabolites between groups were determined by absolute Log1.5FC (fold change). Therapy FDR < 0.05 and fold change > 1.5 were used to identify significantly differential metabolites. The HCA (hierarchical cluster analysis) results of samples and metabolites were presented as heatmaps with dendrograms. HCA was carried out by R package pheatmap. For HCA, normalized signal intensities of metabolites (unit variance scaling) are visualized as a color spectrum. The detailed information of anthocyanins were listed in Table S5.

LUC assay

The LUC assay was performed according to Du et al. (2024a). The promoter sequence of *CAD* and *CHS* were cloned into the reporter effector pGreenII LUC0800 (pLUC-Pro) and the coding sequence of *NAC1* was fused into pGreenII 62SK (pSK-NAC1). The *Agrobacterium* strains (GV3101) were incubated overnight and resuspended in infiltration buffer (20 mM MES, 0.1 mM acetosyringone, and 10 mM $MgCl_2$) and final diluted to the concentration of OD_{600} = 0.6–0.8. Suspensions of pLUC-Pro and pSK-NAC1 were mixed in equal volumes and infiltrated into *Nicotiana benthamiana* leaves. After 48 h, the transformed leaves were sprayed with 0.1 M luciferin solution and kept in the dark for 7 min. A low light-cooled CCD imaging apparatus (Lumazone Pylon 2048 B, Princeton Instruments) was used to capture and analyze the acquired LUC images.

Transient overexpression assay

The open reading frames (ORF) of *NAC1* were cloned using a primer pair containing EcoRI and BamHI sites and ligated to pBIN-eGFP. Then, the positive vector was confirmed using sequencing, and transduced into *Agrobacterium tumefaciens* LBA4404. GFP controls, pBIN-NAC1 was transferred into *Nicotiana benthamiana* using *A. tumefaciens*-mediated method. Four days after infiltration, the representative fruit was collected for further experiments.

Results

UVA, UVAB and UVB altered the proteome patterns of H. vulgare.

To investigate the responses of *H. vulgare* to UVB, UVA and UVA + UVB (UVAB) stresses, three biological replicates for *H. vulgare* from CK, UVB, UVA and UVAB treatments were collected for proteome sequencing. Totally, 3949 proteins were identified in *H. vulgare*. Then, we performed principal component

analysis (PCA) on all proteome profiles to investigate the proteomic pattern of *H. vulgare* following UVB, UVA and UVAB exposures (Fig. 1A). PCA plot was constructed using principal component 1 (PC1) and PC2, which explained 47.8% and 8.1% variations between all samples (Fig. 1A). The PCA plot showed that the samples from CK clearly distributed at a single region and separated with UVB, UVA and UVAB (Fig. 1A), suggesting that all UVB, UVA and UVAB treatments dramatically altered the proteome pattern of *H. vulgare*. Typically, the differences between experimental groups were mainly represented by PC1, while PC2 mainly explained the differences among biological replicates from the same treatment (Fig. 1A). Additionally, UVB samples also clearly separated with UVA, UVAB and CK, and the differences between UVB and CK were more significant than that between UVAB/UVA vs. CK (Fig. 1A), suggesting that *H. vulgare* are more responsive to UVB. Meanwhile, *H. vulgare* exhibited similar responses to UVA and UVB, and the effect of UVA on plant protein expression was minimal that UVA samples were closet to CK (Fig. 1A).

Then, to investigate the detailed changes in proteome of *H. vulgare* following UVA, UVB and UVAB exposures, we analyzed the differentially expressed proteins (DEPs) of all 3949 identified proteins in UVA vs. CK, UVB vs. CK and UVAB vs. CK comparisons based on $P < 0.05$ and Foldchange > 1.5 (Fig. 1B). Totally, 73 DEPs were identified in UVA vs. CK, with 49 downregulated DEPs and 24 upregulated DEPs (Fig. 1B). Additionally, we identified 272 DEPs (228 down- and 44 up-regulated DEPs) in UVAB vs. CK and 678 DEPs (477 down- and 201 up-regulated DEPs) in UVB vs. CK comparison (Fig. 1B). Typically, most DEPs in *H. vulgare* associated with UVA, UVB and UVAB exposures were mainly located in nucleus, cytoplasm, secreted and chloroplast (Fig. 1C). It has been well documented that chloroplast involved in responses of plants to UV by regulating reactive oxygen homeostasis caused by UV stress [32]. Moreover, COG/KOG enrichment showed that most of proteins among the DEPs from these 3 pairwise comparisons mainly involved in RNA processing and modification, Energy production and conversion, Translation, ribosomal structure and biogenesis, Posttranslational modification, protein turnover, chaperones, General function prediction only and Intracellular trafficking, secretion, and vesicular transport (Figure S1). Thus, these results suggested UVA, UVAB and especially UVB could alter the proteome pattern of *H. vulgare*, especially leading changes in levels of proteins located in nucleus, cytoplasm, secreted and chloroplast.

Different wavelengths of UV cause changes in expression of different functional proteins in H. vulgare.

Plants make different responses to different wavelength of light [33]. Here, we investigated the function of DEPs in *H. vulgare* following UVA, UVB and UVAB exposures using gene ontology (GO) enrichment analysis. For UVA vs. CK comparison, 90 GO terms were significantly enriched against all DEPs (Fig. 2A, Table S1). Typically, these DEPs mainly functioned in protein storage vacuole membrane, vacuolar proton-transporting V-type ATPase, plant-type vacuole membrane and post-spliceosomal complex, with thiol-dependent ubiquitin-specific protease activity, ubiquitinyl hydrolase activity, receptor binding, cysteine-type peptidase activity, hydrolase activity, signaling receptor activity, cytokine activity, vascular endothelial growth factor receptor binding, molecular transducer activity, ATPase activity, monocarboxylic acid binding, inositol monophosphate 3-phosphatase activity, ion transmembrane

transporter activity and peptidase activity (Fig. 2A, Table S1). These DEPs associated with UVA mainly involved in regulation of protein complex disassembly, DNA replication checkpoint, DNA damage response, single organism reproductive process, negative regulation of G2/M transition of mitotic cell cycle, DNA integrity checkpoint, glyoxal metabolic process and cell communication (Fig. 2A, Table S1). These results showed that UVA mainly affected proteins involved in DNA replication and cell cycle, which then may cause damage to cell growth in plants.

For UVAB vs. CK comparison, DEPs mainly functioned in ESCRT complex, organelle membrane, endosome, ESCRT I complex and cis-Golgi network in plant cell (Fig. 2B, Table S2). For molecular function, 21 terms were significantly enriched, including protein disulfide oxidoreductase activity, peptidase inhibitor activity, glutathione transferase activity, peroxiredoxin activity, oxidoreductase activity, lipid binding, transferase activity and thioredoxin peroxidase activity (Fig. 2B, Table S2). And these DEPs associated with UVAB mainly involved in 46 biological progresses, especially lipid transport, response to stimulus, endosomal transport, vacuolar transport, positive regulation of macromolecule metabolic process, cell surface receptor signaling pathway, glutathione metabolic process, cell redox homeostasis, response to abscisic acid, glutamate catabolic process and seed development (Fig. 2B, Table S2). Of note, numerous processes relevant to oxidant responses were identified in UVAB vs. CK comparison, including glutathione metabolic process, cell redox homeostasis, response to abscisic acid, glutamate catabolic process, while it also affected proteins relevant to seed development (Fig. 2B, Table S2). It has been found that UV exposure always accompanied by oxidant stress and disordered oxygen-radical homeostasis, leading to damage to plant cell and growth [34]. Thus, these results suggested that UVAB may cause oxidant stress in plant cell to affect seed development.

Subsequently, we analyzed the function of DEPs from UVB vs. CK comparison. The GO results showed that these DEPs mainly distributed in respiratory chain complex, mitochondrial membrane, oxidoreductase complex, mitochondrion, plasma membrane, NADH dehydrogenase complex, chromatin, organellar ribosome, nucleosome and protein-DNA complex (Fig. 2C, Table S3). Typically, these DEPs with functions of voltage-gated channel activity, gated channel activity, transcription corepressor activity, DNA binding, kinase regulator activity, phospholipid transporter activity, sphingolipid binding, ceramide binding and ATPase activity, mainly involved in protein-DNA complex assembly, nucleosome assembly, chromatin assembly, DNA packaging and anthocyanin-containing compound biosynthetic process (Fig. 2C, Table S3). Anthocyanin biosynthesis was the well-documented processes in plants in response to UV stress, anthocyanin could protect plants from oxidant damage caused by UV exposure [35]. Thus, these results suggested that plant could trigger the anthocyanin biosynthesis in response to UVB exposure.

Changes in anthocyanin biosynthesis were the main responses in H. vulgare to UVAB and UVB exposures.

Here, we further performed KEGG pathway enrichment analysis on DEPs from three pairwise comparisons (Fig. 3A). For DEPs from UVA vs. CK, KEGG results showed that these DEPs mainly involved in Phagosome, Vitamin B6 metabolism, Diterpenoid biosynthesis, Oxidative phosphorylation,

Phosphatidylinositol signaling system, Phenylalanine metabolism, Plant hormone signal transduction, Tyrosine metabolism, Protein export and Metabolic pathways (Fig. 3A). In parallel, DEPs from UVAB vs. CK mainly functioned in Glutathione metabolism, Phagosome, Protein processing in endoplasmic reticulum, Valine, leucine and isoleucine biosynthesis, Porphyrin metabolism, Phenylpropanoid biosynthesis, D-Amino acid metabolism, Monoterpenoid biosynthesis, Phenylalanine metabolism, Butanoate metabolism, Thiamine metabolism, Plant hormone signal transduction and 2-Oxocarboxylic acid metabolism (Fig. 3A). In addition, KEGG pathway enrichment analysis on DEPs from UVB vs. CK showed that 8 biosynthesis pathways were significantly enriched, including Oxidative phosphorylation, Plant hormone signal transduction, Anthocyanin biosynthesis, Basal transcription factors, Diterpenoid biosynthesis, Phenylpropanoid biosynthesis, Flavonoid biosynthesis and MAPK signaling pathway (Fig. 3A). Typically, we noted the significant enrichment of anthocyanin and flavonoid biosynthesis in UVB vs. CK (Fig. 3B), reaching a consensus with GO results that UVB could trigger the proteome pattern of flavonoid and anthocyanin biosynthesis in *H. vulgare* (Fig. 3A). Additionally, UVA vs. CK, UVAB vs. CK and UVB vs. CK shared 25 pathways, such as Ribosome, Phagosome, Plant hormone signal transduction, Starch and sucrose metabolism, Biosynthesis of amino acids, Glycolysis / Gluconeogenesis, Protein export, Proteasome, Diterpenoid biosynthesis, Tyrosine metabolism, MAPK signaling pathway and Oxidative phosphorylation (Fig. 3B). Of note, there are 45 pathways were specifically enriched under UVB exposure, especially DNA replication, Glycerophospholipid metabolism, Basal transcription factors, Photosynthesis, Fatty acid degradation, alpha-Linolenic acid metabolism, Aminoacyl-tRNA biosynthesis, Anthocyanin biosynthesis, Fatty acid metabolism, Flavonoid biosynthesis, ABC transporters and Sphingolipid metabolism (Fig. 3B).

Considering the effects of importance of anthocyanin synthesis and antioxidant system in plant in response to UV exposure, we further analyzed the expression of related proteins in *H. vulgare* following UVB, UVAB and UVA exposures. The expression heat map of proteins relevant to antioxidant system showed that the expression levels of most related proteins were higher in *H. vulgare* under UVAB and especially UVB exposures, compared to UVA and CK (Fig. 3C). Meanwhile, the proteins involved in anthocyanin synthesis were also triggered to highly expressed in *H. vulgare* by UVAB and especially UVB exposures, but not UVA (Fig. 3C). Taken together, we proposed that different wavelength of UV could trigger different responses in plants, typically anthocyanin biosynthesis and antioxidant reaction was the main responses in *H. vulgare* to UVB exposure.

UVAB and UVB triggered accumulation of anthocyanins in H. vulgare.

Further, we compared the anthocyanin-related metabolic profiles of *H. vulgare* following UVA, UVAB and UVB exposures. To identify the overview of changes in anthocyanin composition of *H. vulgare* following UVA, UVAB and UVB exposures, we performed PCA analysis on all metabolic profiles of *H. vulgare* (Fig. 4A). The PCA plots constructed by PC 1 and 2 showed significant variations in anthocyanin composition among all groups, while PC1 and PC2 explained 33.2% and 15.4% variations associated with experimental treatments (Fig. 4A). Typically, PC1 mainly explained the variations in anthocyanins compositions of *H. vulgare* caused by UVAB and UVB exposures (Fig. 4A), supporting the involvement of

anthocyanins synthesis of *H. vulgare* in response to UVAB and UVB exposures. Totally, 28 anthocyanins were identified in *H. vulgare* (Fig. 4B, Figure S2). Typically, the contents of most of anthocyanins were higher in *H. vulgare* under UVB exposure in comparison with UVA and CK, including Procyanidin B2, Cyanidin-3-O-sambubioside, Peonidin-3-O-glucoside, Cyanidin-3-O-glucoside, Pelargonidin-3-O-glucoside, Procyanidin B1, Peonidin-3-O-sophoroside, Petunidin-3-O-glucoside, Cyanidin-3-(malonyl)glucoside-5-rhamnoside, Delphinidin-3-O-glucoside, Cyanidin-3-O-sophoroside, Cyanidin-3-O-(6-O-malonyl-beta-D-glucoside), Cyanidin-3,5-O-diglucoside, Cyanidin-3-O-xyloside and Peonidin (Fig. 4B). Of note, the contents of all anthocyanins in *H. vulgare* under UVAB exposure was higher than that in CK and UVA, while UVA did not induce increases of anthocyanins in *H. vulgare* (Fig. 4B). Thus, we concluded that anthocyanins accumulation was the main response in *H. vulgare* to UVAB and UVB exposures.

Active regulation network involved in regulating anthocyanin synthesis in H. vulgare in response to UVB and UVAB exposures.

To identify the hub proteins involved in anthocyanin synthesis in *H. vulgare* in response to UVB and UVAB exposures, we analyzed the correlation between levels of proteins and anthocyanins using Pearson algorithm. The results showed that proteins represented by Q40069, F2D3Q9, F2E8A9, M0WRX0, F2E7V8, F2CXT3 and F2E8K5 were highly correlated with the anthocyanin level in *H. vulgare* (Fig. 5A), implying their involvements in synthesizing anthocyanin in *H. vulgare*. Considering the involvement of anthocyanin synthesis *H. vulgare* in response to UVB and UVAB exposures, we further constructed the co-expression network of proteins (Q40069, F2D3Q9, F2E8A9, M0WRX0, F2E7V8, F2CXT3 and F2E8K5) relevant to anthocyanin synthesis using WGCNA based on all proteome profiles of *H. vulgare* (Fig. 5B-D). The expression data of all transcription factors and kinases of *H. vulgare* were selected via Nr annotation for WGCNA construction. We set the soft threshold to 26 (R^2 = 0.85) to construct a scale-free network (Figure S3A). Then, 9 modules were identified by hierarchical clustering and the dynamic branch cutting, each module was assigned a unique color as an identifier (Fig. 5B, C, Figure S3B). Then, the modules highly correlated with the related traits were filtered out for further construction of regulation network of anthocyanin synthesis in *H. vulgare* (Fig. 5C). Based on the WGCNA results, we identified that MEbrown, MEyellow and MEturquoise were highly related to proteins relevant to anthocyanin synthesis (Fig. 5C). Among proteins from these modules, we constructed the co-expression regulation networks for anthocyanin synthesis in *H. vulgare* (Fig. 5D). Totally, we identified that 4 transcription factors and 34 kinases were responsible for positively regulating anthocyanin synthesis in *H. vulgare* in response to UVB and UVAB exposures ($P < 0.05$, Fig. 5D). As shown in Fig. 5D, A0A8I6WJ93, A0A8I6WLA6, A0A8I7B6M6 and especially F6IAY3 (NAC transcription factor) were the hub transcription factors involved in the regulation network of anthocyanin synthesis in *H. vulgare*, and it was positively correlated with the expression of anthocyanin-related proteins (Fig. 5D). Of note, most of these regulators were upregulated to higher expression levels in *H. vulgare* by UVAB and UVB exposures, supporting their involvements in regulating responses in *H. vulgare* to UVAB and UVB exposures (Fig. 5D). Further RT-qPCR assay confirmed that transcription factors including A0A8I6WJ93, A0A8I6WLA6, A0A8I7B6M6 and especially F6IAY3 were activated to upregulate in *H. vulgare* by UVAB and UVB exposures, but not UVA (Fig. 5E). Of note, LUC assay confirmed that NAC1 could directly bind on the promoters of *CAD1* and

CHS to trigger their expression (Fig. 5F). Further transient overexpression assay showed that *NAC1* overexpression activated expression of *CHS*, *CAD* and *ANS* in plants, supporting its function in activating anthocyanin biosynthesis in *H. vulgare* (Fig. 5G). Taken together, these results suggested that the UVAB/UVB-reprogrammed anthocyanin synthesis in *H. vulgare* was regulated by a complex network.

Discussion

In the plateau region, especially Qinghai-Tibet Plateau, UV stress has become a nonnegligible obstacle to the development of crops. Thus, it is of great practical significance to investigate the detailed plant responses to UV exposures for guiding the agriculture development in these regions. Presently, we found that UVA, UVAB and UVB reprogrammed the proteome pattern of *H. vulgare*. In detail, UVA mainly affected the expression of proteins involved in cell cycle and DNA repair, while UVB and UVAB mainly altered proteins involved in anthocyanin biosynthesis and antioxidant systems. Typically, all identified proteins involved in anthocyanin biosynthesis were activated to upregulate in *H. vulgare* by UVB and UVAB exposures. Further anthocyanin profiles showed that UVB and UVAB caused accumulation of anthocyanin in *H. vulgare*, which may protect *H. vulgare* from UV-associated oxidant damage to plant cell. Then, we constructed the network for regulating UV-triggered anthocyanin biosynthesis in *H. vulgare* using proteome profiles. Importantly, we identified NAC transcription together with numerous kinases were responsible for regulating UVAB/UVB-triggered anthocyanin biosynthesis in *H. vulgare*. Of note, NAC1 directly bound on the promoters of *CAD1* and *CHS* to trigger their expression, then activated anthocyanin biosynthesis in *H. vulgare*. Overall, our research depicted the detailed global responses of *H. vulgare* to UV challenge, which contributed to our understanding of adaptive mechanisms of plants in plateau.

With the destruction of the ozone layer, the research on ultraviolet radiation has attracted increasing attention. Ultraviolet-B radiation is a light wave with a wavelength between 280 and 320 nm, and its high energy can directly lead to DNA strand breakage and blocked cross-linked replication between DNA strand and DNA strand or protein [36, 37]. Meanwhile, UV exposure also caused the disruption and structural changes of polypeptide chains in protein molecules in plants and changes in multiple metabolic activities of organisms [38]. Similarly, we found that the UVA could affected the expression of proteins involved in cell cycle and DNA replications. In addition, UV-B can also trigger the accumulation of reactive oxygen species, resulting in lipid peroxidation of biofilm [39], then change the fluidity and permeability of the membrane and affecting a variety of physiological activities of organisms [40]. UV-B radiation can directly or indirectly affect the synthesis, accumulation and metabolism of primary metabolism and secondary metabolites in plants [11]. Of note, combining with metabolomics, genomics and proteomics provides theoretical basis and technical support for the application of UV-B radiation in agricultural production and agricultural product processing. Since UV-B irradiation can induce oxidative stress in plants, the biosynthesis pathway of antioxidant active substances such as polyphenols and flavonoids will be activated, so as to rapidly synthesize a large number of antioxidant active substances to effectively repair the body damage caused by oxidative stress [41, 42]. Polyphenols are a class of compounds formed by the substitution of polyhydroxyl groups on the basic skeleton of phenol. They are

important bioactive substances in human diet and secondary metabolites closely related to plant defense mechanisms [43]. A large number of studies have shown that that UVB treatment can significantly increase flavonoid and anthocyanin content in plant tissues [44–46]. Here, we also found that UV-B is an important factor in inducing the biosynthesis of plant anthocyanins, while UVA + UVB also could promote the anthocyanin accumulation in *H. vulgare*. Anthocyanins and flavonoid metabolites have efficient scavenging function of reactive oxygen species [42]. Typically, both low and high doses of UV-B radiation lead to an increase in ROS in the plant [47]. Therefore, the accumulation of anthocyanin metabolites may be an important way for plants to resist strong UV stress at high altitude.

Because anthocyanins and flavonoids metabolites not only help plants resist abiotic and biological stresses, they are also important nutrients in crops [48]. Therefore, the rational use of ultraviolet rays can be used as an important means of metabolic regulation in agricultural production, so as to improve crop yield and carry out targeted regulation and accumulation of target products. It was found that phenylpropanoid-derived flavonoid and anthocyanin biosynthesis was mainly regulated by MYB transcription factors to perform related function in plant [30]. Of note, we identified NAC transcription factor as regulator for mediating UV-associated anthocyanin biosynthesis via constructing regulation network of anthocyanin biosynthesis in *H. vulgare*. And the detailed regulation mechanism of NAC in mediating UV-associated anthocyanin biosynthesis in *H. vulgare* will be the focus in our future work. Overall, the study on the effects of UV-B on the main nutrients and bioactive substances in plants is of great significance for guiding agricultural production, especially for the directed regulation of specific nutrients and bioactive substances in agricultural products.

Conclusion

In the present study, we deciphered the global responses of *H. vulgare* to UV challenge via integrating metabolome and proteome. we found that UVA, UVAB and UVB reprogrammed the proteome pattern of *H. vulgare*. UVA mainly affected the expression of proteins involved in cell cycle and DNA repair. In addition, UVB and UVAB mainly activated proteins involved in anthocyanin biosynthesis and antioxidant systems, leading to accumulation of anthocyanin in *H. vulgare* to protect *H. vulgare* from UV-associated oxidant damage. Of note, we identified that NAC transcription together with numerous kinases were responsible for regulating UVAB/UVB-triggered anthocyanin biosynthesis in *H. vulgare.* Thus, the present study gain insight into the adaptive mechanisms of plants in plateau.

Declarations

Author Contributions: Z.H.: writing-original draft, writing-review and editing. T.Z.: data curation, visualization, methodology. X.Y. and C.DJ: methodology, software. Y.Z.: formal analysis, validation, conceptualization. X.W. and C.D: supervision, funding acquisition. Y.L. and T.Z.: resources, supervision, funding acquisition. All authors have read and agreed to the published version of the manuscript.

Funding: This work was supported by Natural Science Funds of Xizang (XZ202101ZR0073G).

Ethics approval and consent to participate

The collection of plant materials used in our study complied with permission of related institutions, and complied with national or international guidelines and legislation. The experiments did not involve endangered or protected species.

Consent for publication

Not applicable.

Institutional Review Board Statement: Not applicable.

Informed Consent Statement: Not applicable.

Data Availability Statement: The data reported in this paper have been deposited in the OMIX, China National Center for Bioinformation / Beijing Institute of Genomics, Chinese Academy of Sciences (https://ngdc.cncb.ac.cn/omix: accession no.OMIX009895).

Conflicts of Interest: The authors declare no conflicts of interest.

References

1. Huang R, Gao HY, Liu J, Li XP. WRKY transcription factors in moso bamboo that are responsive to abiotic stresses. J Plant Biochem Biotechnol. 2022;31:107–14.
2. Kataria S, Jajoo A, Guruprasad KN. Impact of increasing Ultraviolet-B (UV-B) radiation on photosynthetic processes. J Photochem Photobiol B. 2014;137:55–66.
3. Hegglin MI, Shepherd TG. Large climate-induced changes in ultraviolet index and stratosphere-to-troposphere ozone flux. Nat Geosci. 2009;2:687–91.
4. Zhang H, Wu S, Huang Y, Wang Y. Effects of stratospheric ozone recovery on photochemistry and ozone air quality in the troposphere. Atmos Chem Phys. 2014;14:4079–86.
5. Stapleton AE. Ultraviolet radiation and plants: burning questions. Plant Cell. 1992;4:1353–8.
6. Hollósy F. Effects of ultraviolet radiation on plant cells. Micron. 2002;33:179–97.
7. Larson RA, Garrison WJ, Carlson RW. Differential responses of alpine and non-alpine *Aquilegia* species to increased ultraviolet-B radiation. Plant Cell Environ. 2010;13:983–7.
8. Gwynn-Jones D, Callaghan JALV. Effects of enhanced UV-B radiation and elevated carbon dioxide concentrations on a sub-arctic forest heath ecosystem. Plant Ecol. 1997;128:242–9.
9. Korpelainen H, He Y, Xuan Z, Yao Y, Li C, Li Y. Effects of ultraviolet-B radiation on crop growth, development, yield and leaf pigment concentration of tartary buckwheat (*Fagopyrum tataricum*)

under field conditions. Eur J Agron. 2006;25:215–22.

10. Urban O, TMa I, Holub P, Marek MV. Photosynthesis and growth response of *Calamagrostis arundinacea* and *C. villosa* to enhanced UV-B radiation. Photosynthetica. 2006;44:215–20.
11. Liang T, Yang Y, Liu H. Signal transduction mediated by the plant UV-B photoreceptor UVR8. New Phytol. 2019;221:1247–52.
12. Krupa SV. Ultraviolet-B radiation, ozone and plant biology. Environ Pollut. 2000;110:193–4.
13. Holopainen JK. Can forest trees compensate for stress-generated growth losses by induced production of volatile compounds? Tree Physiol. 2011;31:1356–77.
14. Jansen MAK, Hectors K, O'Brien NM, Guisez Y, Potters G. Plant stress and human health: do human consumers benefit from UV-B acclimated crops? Plant Sci. 2008;175:449–58.
15. Salama HM, Watban AA, Al-Fughom AT. Effect of ultraviolet radiation on chlorophyll, carotenoid, protein and proline contents of some annual desert plants. Saudi J Biol Sci. 2011;18:79–86.
16. Morales LO, Tegelberg R, Brosché M, Keinanen M, Lindfors A, Aphalo PJ. Effects of solar UV-A and UV-B radiation on gene expression and phenolic accumulation in *Betula pendula* leaves. Tree Physiol. 2010;30:923–34.
17. Doma M, Abhayankar G, Reddy VD, Kishor PBK. Carbohydrate and elicitor enhanced withanolide (withaferin A and withanolide A) accumulation in hairy root cultures of *Withania somnifera* (L). Indian J Exp Biol. 2012;50:484–90.
18. Du Y, Ma H, Liu Y, Gong R, Lan Y, Zhao J, Liu G, Lu Y, Wang S, Jia H, Li N, Zhang R, Wang J, Sun G. Major quality regulation network of flavonoid synthesis governing the bioactivity of black wolfberry. New Phytologist. 2024a; 242: 558–575.
19. Stapleton AE. Ultraviolet radiation and plants: burning questions. Plant Cell. 1992;4:1353–8.
20. Bidart-Bouzat MG, Imeh-Nathaniel A. Global change effects on plant chemical defenses against insect herbivores. J Integr Plant Biol. 2008;50:1339–54.
21. Park JS, Kim JB, Cho KJ, Cheon CI, Sung MK, Choung MG, Roh KH. Arabidopsis R2R3-MYB transcription factor AtMYB60 functions as a transcriptional repressor of anthocyanin biosynthesis in lettuce (*Lactuca sativa*). Plant Cell Rep. 2008;27:985–94.
22. Kumari R, Agrawal SB, Supplemental. UV-B induced changes in leaf morphology, physiology, and secondary metabolites of an Indian aromatic plant *Cymbopogon citratus* (D.C.) Staph under natural field conditions. Int J Environ Stud. 2010;67:655–75.
23. Liu ML, Cao B, Zhou SH, Liu YB. Responses of the flavonoid pathway to UV-B radiation stress and the correlation with the lipid antioxidant characteristics in the desert plant *Caryopteris mongolica*. Acta Ecol Sin. 2012;32:150–5.
24. Takshak S, Agrawal SB. Secondary metabolites and phenylpropanoid pathway enzymes as influenced under supplemental ultraviolet-B radiation in *Withania somnifera* Dunal, an indigenous medicinal plant. J Photochem Photobiology B Biology. 2014;140:332–43.

25. Broun P. Transcription factors as tools for metabolic engineering in plants. Curr Opin Plant Biol. 2004;7:202–9.
26. Ohnishi T, Takahashi A, Takeda K. Licht-induced anthocyanin reduces the extent of damage to DNA in UV-irradiated Centaurea cyanus cells in culture. Mutat Research/Environmental Mutagen Relat Subj. 1992;272:277–277.
27. Cheng L, Zhang K, Qing Y, Li D, Cui M, Jin P, Xu T. Proteomic and lipidomic analysis of exosomes derived from ovarian cancer cells and ovarian surface epithelial cells. J Ovarian Res. 2020;13(1):9.
28. Ye J, Fang L, Zheng H, Zhang Y, Chen J, Zhang Z, Wang J, Li S, Li R. Bolund, L. WEGO: A web tool for plotting GO annotations. Nucleic Acids Research. 2006; 34: W293–W297.
29. Kanehisa M, Goto SKEGG. Kyoto Encyclopedia of Genes and Genomes. Nucleic Acids Res. 2000;27:29–34.
30. Du Y, Jia H, Yang Z, Wang S, Liu Y, Ma H, Liang X, Wang B, Zhu M, Meng Y, Gleason ML, Hsiang T, Noorin S, Zhang R. Sun, G. Sufficient coumarin accumulation improves apple resistance to *Cytospora mali* under high-potassium status. Plant Physiol. 2023;192:1396–419.
31. Smith CA, Want EJ, O'Maille G, Abagyan R, Siuzdak GXCMS. Processing mass spectrometry data for metabolite profiling using nonlinear peak alignment, matching, and identification. Anal Chem. 2006;78:779–87.
32. Zhu Y, Wang H, Xiang X, Hayat K, Wu R, Tian J, Zheng H, Xie M, Li B, Du S. A dose-dependent effect of UV-328 on photosynthesis: Exploring light harvesting and UV-B sensing mechanisms. J Hazard Mater. 2024;15:473.
33. Liang Y, Weng X, Ling H, Mustafa G, Yang B. Lu, N. Transcriptomic Insights into Molecular Response of Butter Lettuce to Different Light Wavelengths. Plants (Basel). 2024;13:1582.
34. Chen Z, Dong Y, Huang X. Plant responses to UV-B radiation: signaling, acclimation and stress tolerance. Stress Biology. 2022;2:51.
35. Zhou J, Meng J, Zhang S, Chi R, Wang C, Wang D, Li H. The UV-B-Induced Transcription Factor HY5 Regulated Anthocyanin Biosynthesis in *Zanthoxylum bungeanum*. Int J Mol Sci. 2022;23:2651.
36. Takahashi M, Teranishi M, Ishida H, Kawasaki J, Takeuchi A, Yamaya T, Watanabe M, Makino A, Hidema J. Cyclobutane pyrimidine dimer (CPD) photolyase repairs ultraviolet-B-induced CPDs in rice chloroplast and mitochondrial DNA. Plant J. 2011;66:433–42.
37. Mesa R, Bassnett S. UV-B-induced DNA damage and repair in the mouse lens. Invest Ophthalmol Vis Sci. 2013;54:6789–97.
38. Zlatev ZS, Lidon FJC, Kaimakanova M. Plant physiological responses to UV-B radiation. Emirates J Food Agric. 2012;24:481–501.
39. Bhaskaran J, Panneerselvam R. Accelerated reactive oxygen scavenging system and membrane integrity of two Panicum species varying in salt tolerance. Cell Biochem Biophys. 2013;67:885–92.
40. Krasylenko YA, Yemets AI, Sheremet YA, Blume YB. Nitric oxide as a critical factor for perception of UV-B irradiation by microtubules in Arabidopsis. Physiol Plant. 2012;145:505–15.

41. Eichholz I, Huyskens-Keil S, Keller A, Ulrich D, Kroh LW, Rohn S. UV-B-induced changes of volatile metabolites and phenolic compounds in blueberries (*Vaccinium corymbosum* L). Food Chem. 2011;126:60–4.
42. Du Y, Liu G, Jia H, Liu Y, Tan Y, Wang S, Mu J, Yu J, Xue K, Zhang R, Gleason ML, Liang X, Sun G. Changes in planta K nutrient content altered the interaction pattern between *Nicotiana benthamiana* and *Alternaria longipes*. Plant Cell Environ. 2024b; 15.
43. Fang F, Tang K, Huang WD. Changes of flavonol synthase and flavonol contents during grape berry development. Eur J Food Res Technol. 2013;237(4):529–40.
44. Gondor OK, Szalai G, Kovács V, Janda T, Pál M. Impact of UV-B on drought- or cadmium-induced changes in the fatty acid composition of membrane lipid fractions in wheat. Ecotoxicol Environ Saf. 2014;108:129–34.
45. Mishra V, Mishra P, Srivastava G, Prasad SM. Effect of dimethoate and UV-B irradiation on the response of antioxidant defense systems in cowpea (*Vigna unguiculata* L.) seedlings. Pestic Biochem Physiol. 2011;99:118–23.
46. Teramura AH, Sullivan JH, Lydon J. Effects of UV-B radiation on soybean yield and seed quality: a 6-year field study. Physiol Plant. 1990;80:5–11.
47. Hideg E, Jansen MA, Strid A, UV-B exposure. ROS, and stress: inseparable companions or loosely linked associates? Trends Plant Sci. 2013;18:107–15.
48. Kozłowska A, Szostak-Wegierek D. Flavonoids–food sources and health benefits. Rocz Panstw Zakl Hig. 2014;65:79–85.

Figures

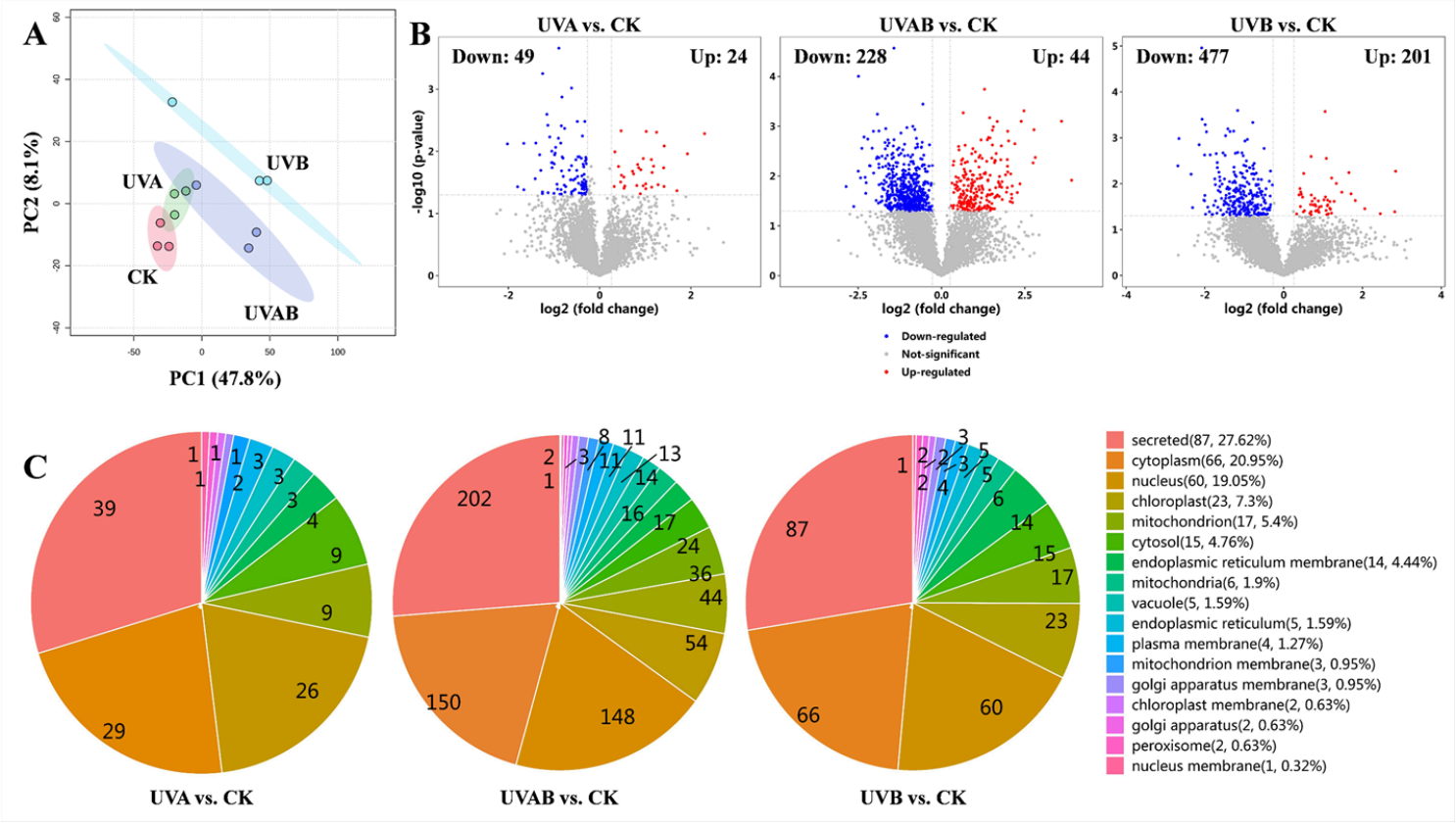

Figure 1

UVA, UVB and UVAB altered the global proteome pattern of *H. vulgare*.

A, D: PCA scores plot of the samples showing distinct separation between UVA, CK, UVB and UVAB at proteome levels. The ellipse represents the 95% confidence interval. **B:** Volcano plot shows the differential proteins (DEPs) with log1.5fold changed ≥ 1.0 and P ≤ 0.05 in UVA vs. CK, UVAB vs. CK and UVB vs. CK pairwise comparisons. The upregulated proteins are shown in red, while the downregulated ones are shown in blue. **C:** Subcellular location analysis on DEPs of *H. vulgare* from each comparison.

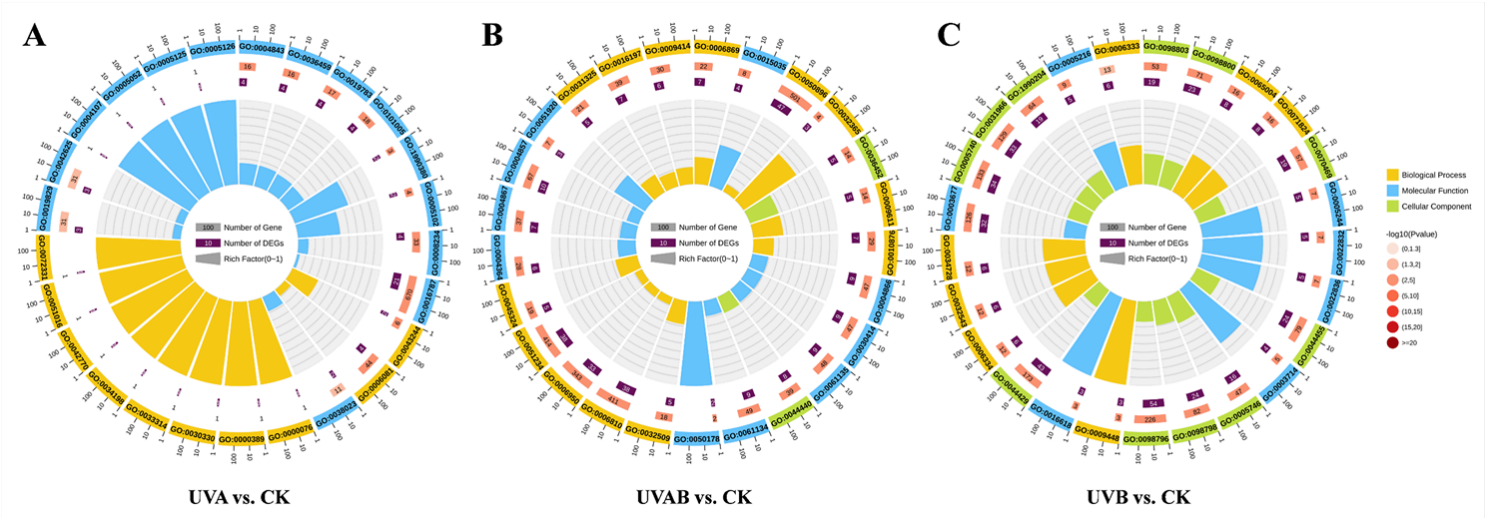

Figure 2

UVA, UVAB and UVB altered the expressions of proteins of *H. vulgare* with different function.

A-**C:** Gene ontology (GO) enrichment analysis on DEPs from UVA vs. CK (A), UVAB vs. CK (B) and UVB vs. CK (C) pairwise comparisons. The various color levels displayed different levels of significance of metabolic pathways from low (green) to high (red). The terms of cellular component, molecular function and biological progress are shown in green, blue and orange, respectively.

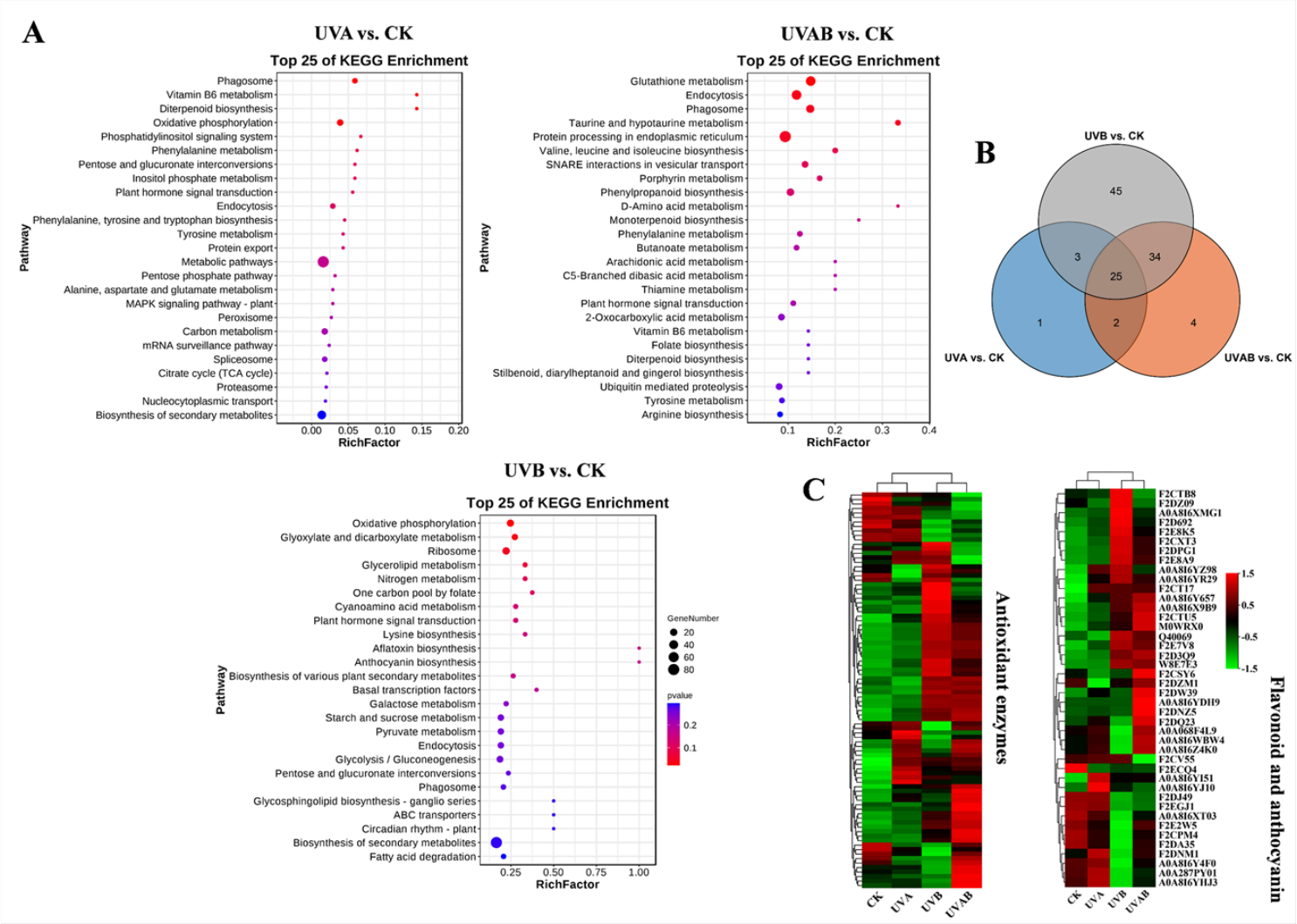

Figure 3

UVB and UVAB triggered the expression of proteins involved in anthocyanin synthesis and antioxidant systems in *H. vulgare*.

A:Scatter plot of the most enriched KEGG pathways of all DEPs from UVA vs. CK, UVAB vs. CK and UVB vs. CK pairwise comparisons. The size and color of each plots represented the protein number and significance of each related pathways. The x-axis represents the rich factor of each pathway. Rich factor was generated by summation of importance measures of matched proteins to all proteins present within the pathway. **B:** Venn diagram displays the overlap of pathways among UVA vs. CK, UVAB vs. CK and UVB vs. CK pairwise comparisons. **C:** Heat maps of the relative expression abundances of proteins in *H.*

*vulgare*following UVA, UVAB and UVB exposures. The scale bar showed the mean values of proteins in each group.

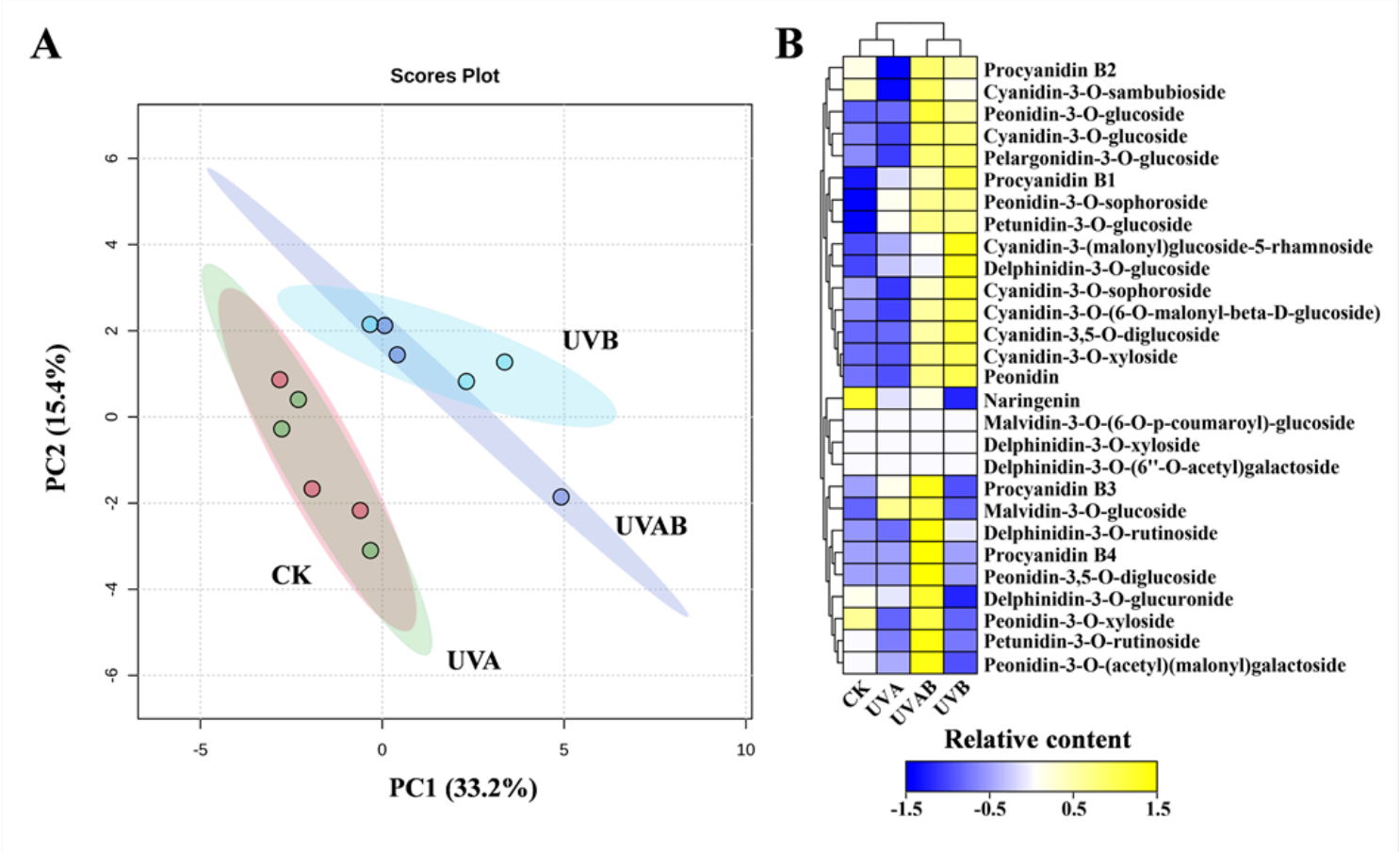

Figure 4

MT activated the regulation network for zeatin synthesis in ENG to enhance its cold tolerance.

A: PCA plots displays the separation of all treatments based on anthocyanin composition and stability of replicates with the same treatment. Each circle represents a sample, the circles labeled by same color were the samples with the same treatment. PCA plots are constructed using top 2 principal component. The ellipse represents the 95% confidence interval. **B:** Heatmap displays the levels of related anthocyanins in *H. vulgare* following UVA, UVAB and UVB exposures. The high and low expression levels of metabolites in each biological replicate are shown in blue and yellow, respectively.

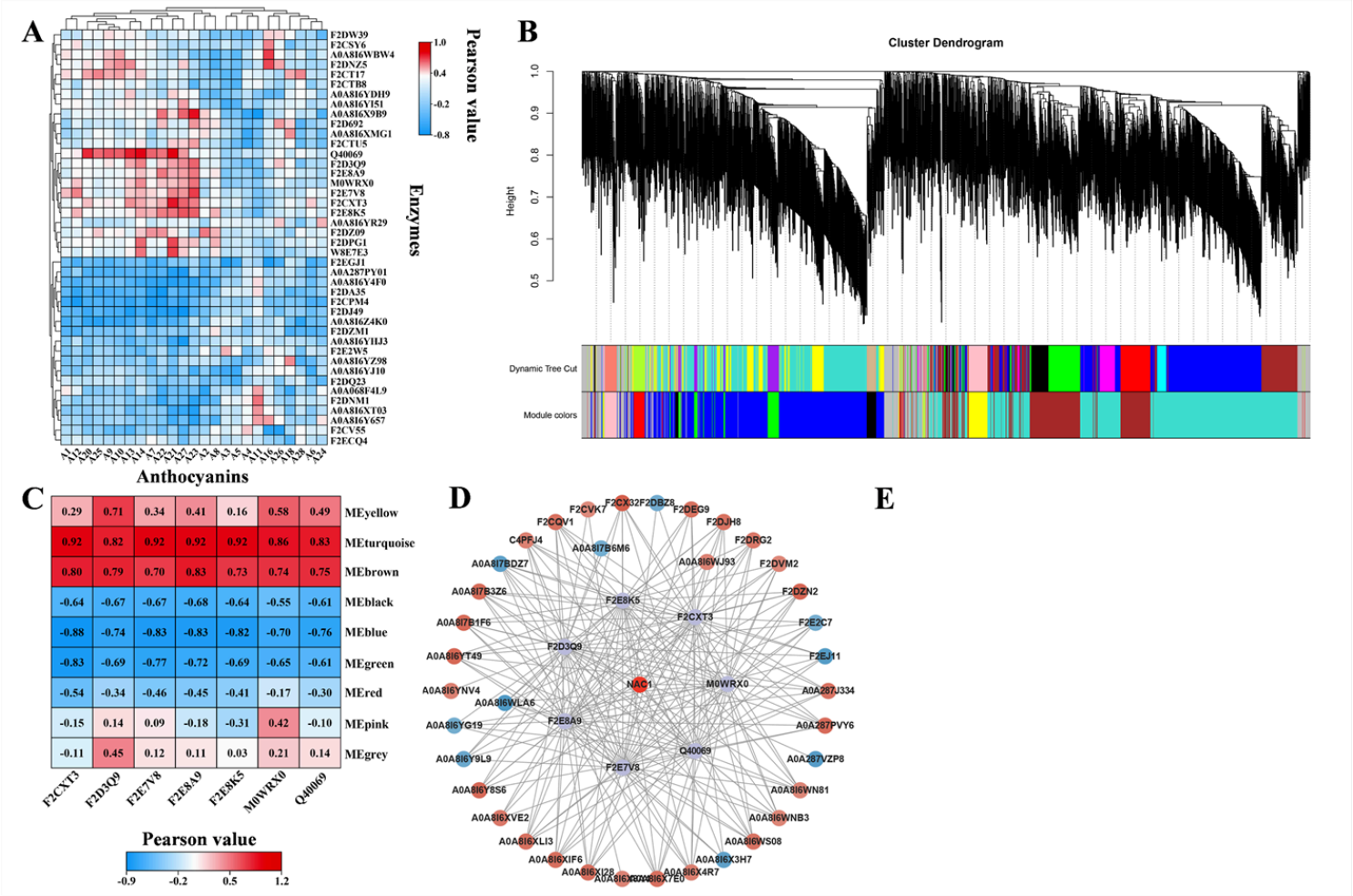

Figure 5

Complex regulation network involved in mediating the anthocyanin responses in *H. vulgare* to UVB exposure.

A: Correlation analysis between proteins responsible for anthocyanin synthesis and anthocyanins in *H. vulgare*following UVA, UVAB and UVB exposures. **B:** Association between modules and experiment trait. The darker the module color, the more significant their relationship. **C:** Heatmap displaying the Module-trait relationships. Each row represents a module eigengene, and column represents a trait. Each cell contains the corresponding correlation and p value. The table is color-coded by correlation based on the color legend. **D:**The weight network of the significant genes involved in the module labeled by MEblack. The color and the size of the circle represented the weight value of each protein in the network. The circle sizes displayed the degree value of corresponding genes in the network, which showed the gene importance. **E:** RT-qPCR detects the expression levels of genes encoding hub transcription factors in *H. vulgare* following UVA, UVAB and UVB exposures, “Different letters represented significance based on P < 0.01 from Student’s T-test”. **F:** LUC report assay detects the binding affinity of NAC1 on promoters of genes encoding anthocyanin biosynthesis. **G:** RT-qPCR determines the expression levels of genes involved in anthocyanin biosynthesis in plant overexpressing *NAC1*. GFP controls, pBIN-NAC1 was transferred into *N.benthamiana* using *A. tumefaciens*-mediated method.

Supplementary Files

This is a list of supplementary files associated with this preprint. Click to download.

- TableS1.xlsx
- TableS2.xlsx
- TableS3.xlsx
- TableS4.xlsx
- TableS5.xlsx
- Supplementalfigures.docx